

## FEATURE ARTICLE

10.1002/2014SW001132

## Supporting Information:

- Readme
- Data Set S1

## Citation:

Frissell, N. A., E. S. Miller, S. R. Kaeppler, F. Ceglia, D. Pascoe, N. Sinanis, P. Smith, R. Williams, and A. Shvokoplyas (2014), Ionospheric Sounding Using Real-Time Amateur Radio Reporting Networks, *Space Weather*, 12, doi:10.1002/2014SW001132.

Accepted article online 22 OCT 2014

## Ionospheric Sounding Using Real-Time Amateur Radio Reporting Networks

N. A. Frissell, E. S. Miller, S. R. Kaeppler, F. Ceglia, D. Pascoe, N. Sinanis, P. Smith, R. Williams, and A. Shvokoplyas

**Abstract** Amateur radio reporting networks, such as the Reverse Beacon Network (RBN), PSKReporter, and the Weak Signal Propagation Network, are powerful tools for remote sensing the ionosphere. These voluntarily constructed and operated networks provide real-time and archival data that could be used for space weather operations, forecasting, and research. The potential exists for the study of both global and localized effects. The capability of one such network to detect space weather disturbances is demonstrated by examining the impacts on RBN-observed HF propagation paths of an X2.9 class solar flare detected by the GOES 15 satellite. Prior to the solar flare, the RBN observed strong HF propagation conditions between multiple continents, primarily Europe, North America, and South America. Immediately following the GOES 15 detection of the solar flare, the number of reported global RBN propagation paths dropped to less than 35% that of prior observations. After the flare, the RBN showed the gradual recovery of HF propagation conditions.

### Introduction

Space weather and its ionospheric effects can significantly impact many important modern technological systems, including high-frequency communication networks, Global Navigation Satellite Systems (e.g., the Global Positioning System/GPS), over-the-horizon radars, and power distribution grids. Often, these impacts adversely affect the systems listed above; and therefore, substantial efforts have been made to measure, characterize, and model the ionosphere. These characterizations and models are then used to mitigate the adverse effects of space weather dynamics. Spatially and temporally dense global ionospheric measurements are critically important for real-time operations, forecasting, and basic space weather and scientific research [Schunk *et al.*, 2014].

A variety of instrument networks currently provide data for ionospheric characterization, including networks of ionosondes [Reinisch *et al.*, 2005], GPS total electron content (TEC) receivers [Rideout and Coster, 2006], satellite-based GPS occultation receivers [Coster and Komjathy, 2008], incoherent scatter radars [Eccles *et al.*, 2011], and high-frequency radars [Chisham *et al.*, 2007]. However, the ionosphere is global in size, complex and structured at local spatial scales, and highly dynamic. Although the aforementioned instrument networks are extensive, the ionospheric system remains undersampled. A new source of measurements would be a welcome addition to the current ensemble of ionospheric monitoring networks.

Recently, radio amateurs have voluntarily built networks which monitor transionospheric radio links in real time and report these observations back to central servers. Amateur radio operators, also known as ham radio operators, are radio hobbyists who are licensed to conduct two-way communications on amateur radio frequencies for noncommercial purposes. The amateur radio bands are distributed across the entire radio spectrum, including those bands which support long-distance propagation and are directly impacted by ionospheric conditions. Table 1 lists the most active of these amateur frequencies, which are spread across the MF (medium frequency, 300 kHz–3 MHz), HF (high frequency, 3–30 MHz), and VHF (very high frequency, 30–300 MHz) bands.

Radio amateurs routinely use these frequencies to attempt two-way communications with distant locations in an activity known as “DXing.” Activity is increased during “contest” periods, in which operators engage in a time-limited competition to exchange a prescribed minimum amount of information with as many fellow amateurs in as many places as possible. These activities, among others, provide a geographically diverse source of signals across the radio spectrum. These links may be viewed as ionospheric “soundings,” and give

**Table 1.** Amateur Radio Bands Typically Monitored for Propagation Conditions<sup>a</sup>

Approximate Wavelength (m)	Frequency (MHz)
160	1.800–2.000
80	3.500–4.000
40	7.000–7.300
30	10.100–10.150
20	14.000–14.350
17	18.068–18.168
15	21.000–21.450
12	24.890–24.990
10	28.000–29.700
6	50.000–54.000
2	144.000–148.000

<sup>a</sup>Frequency limits listed here are valid in the United States; exact frequency limits will vary based on country.

valuable information when reported back to a central database and properly analyzed. In this article, we describe some amateur radio reporting networks that are currently operational and provide an example of an X-class solar flare impacting the signals monitored by these networks.

### Amateur Radio Reporting Network Architecture

Multiple amateur radio reporting networks currently exist, each with its own characteristics and strengths. Table 2 gives the names, Internet addresses, and summary notes for a

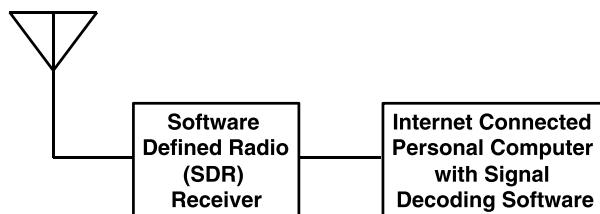
selection of popular networks. The oldest network, the DX Cluster, relies on manual reports provided by operators listening to radios. WSPRNet, the Weak Signal Propagation Reporting Network, is a digital mode specifically designed for ionospheric propagation monitoring [Taylor and Walker, 2010]. Both PSKReporter and the Reverse Beacon Network (RBN) use passive receivers to automatically identify signals. PSKReporter monitors numerous digital communication modes, including phase shift keying 31 Hz (PSK31) and radioteletype (RTTY), while the RBN primarily focuses on Morse code (also known as Continuous Wave/CW) signals. The RBN and PSKReporter are advantageous in that the receiving stations are fully automatic and may be legally operated by users without amateur radio licenses.

Figure 1 shows a block diagram of the hardware for a typical RBN or PSKReporter-type receiving station, including the antenna, receiver, and computer. An ideal station would be able to receive signals omnidirectionally and simultaneously with equal response across all bands of interest (typically 1.8–54 MHz). Recent advances in software-defined radio (SDR) have made this nearly possible through direct digital sampling and software decoding of large portions of the radio frequency (RF) spectrum. Antennas and SDR receivers which meet the required specifications are available commercially. Once the RF spectrum has been sampled by the SDR and sent to the computer, further processing must be done in order to identify the signals of interest.

The RBN relies on a multiband, multichannel Morse code decoding program (CW Skimmer, developed by coauthor Alex Shovkopyas) to decode all observed Morse code transmissions in parallel and report data

**Table 2.** Selected Real-Time Amateur Radio Reporting Networks

Network Name and Address	Network Description
Reverse Beacon Network <a href="http://www.reversebeacon.net/">http://www.reversebeacon.net/</a>	Passive receiving stations automatically listen primarily for Morse code transmissions.
WSPRNet <a href="http://wsprnet.org/">http://wsprnet.org/</a>	Weak Signal Propagation Reporting Network. This is an active mode specifically designed for evaluating ionospheric communication links. Member stations typically transmit and receive.
PSKReporter <a href="http://pskreporter.info/">http://pskreporter.info/</a>	Passive receiving stations automatically listen for digital amateur radio transmissions, including phase shift keying 31 Hz (PSK31), radioteletype (RTTY), and many others.
DX Cluster e.g., <a href="http://www.dxwatch.com/">http://www.dxwatch.com/</a>	Network where radio operators manually report on stations they have contacted and heard. This is the oldest digital amateur reporting network; it remains active today.



**Figure 1.** Block diagram for a typical automatic amateur reporting network receiving station, including the antenna, receiver, and computer. An ideal station would be able to receive signals omnidirectionally and simultaneously with equal response across all bands of interest (typically 1.8–54 MHz). Antennas and SDR receivers which meet the required specifications are available commercially.

back to the RBN servers. Figure 2 is a screenshot of the CW Skimmer program which shows the decoding of a 3 kHz segment of the 40 m amateur radio band. The left-hand portion of the screenshot shows a waterfall display, which is a short-time Fourier transform that plots spectral power versus time. Current signals appear at the right edge of the waterfall and move to the left with time. Visual representations of the Morse code signals detected can be observed in the waterfall. CW Skimmer uses a

Bayesian statistics-based algorithm for decoding each signal. The amateur radio call sign associated with each signal is displayed in the right-hand column of the window, and the latitude and longitude of each station may be determined via a call sign lookup in an appropriate database.

For the purpose of showing detail, Figure 2 shows only 3 kHz of spectrum. This is the standard audio pass-band of a typical analog amateur radio receiver. However, the most capable software-defined radio receivers and computers (as described above) would process all HF spectrum of interest simultaneously.

### Case Study: Ionospheric Impacts of the 13 May 2013 Solar Flare

We demonstrate the capabilities of these amateur radio networks to observe the ionospheric effects of a space weather event by showing the impact of an X-class solar flare observed by the Geostationary Operational Environmental Satellite (GOES) 15 spacecraft on observations made by the Reverse Beacon Network (RBN). All data analysis and visualization of RBN and GOES data were completed with the help of free, open source software tools such as matplotlib [Hunter, 2007], IPython [Pérez and Granger, 2007], pandas [McKinney, 2010], and others [e.g., Millman and Aivazis, 2011]. Figure 3 shows both Reverse Beacon Network and GOES 15 data from 13 May 2013. Figures 3a–3d show maps of observations made by the RBN

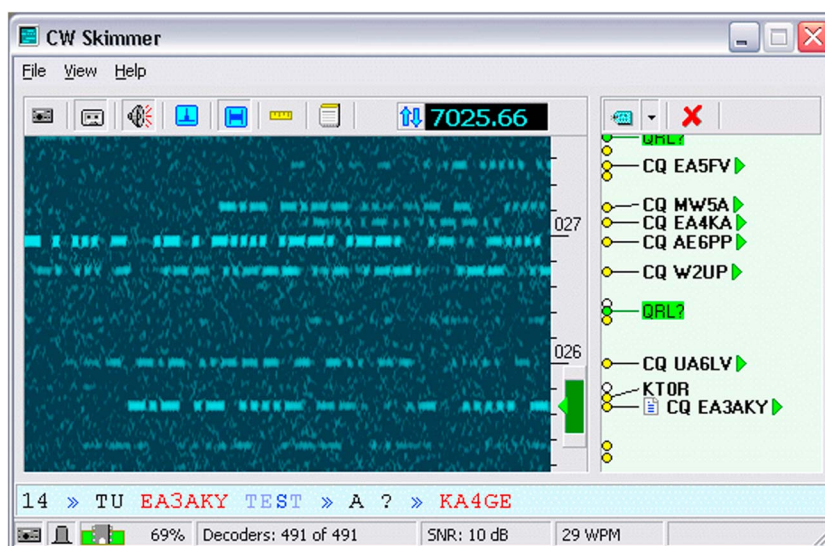


**Figure 2.** A screenshot of the CW Skimmer program used by the Reverse Beacon Network shown decoding a 3 kHz segment of the 40 m amateur radio band. The left-hand portion of the screenshot shows a waterfall display, which is a short-time Fourier transform that plots spectral power versus time. Visual representations of the Morse code signals can be observed in the waterfall. The right-hand column of the screenshot shows a list of radio call signs detected by the CW Skimmer Morse code decoding algorithm.

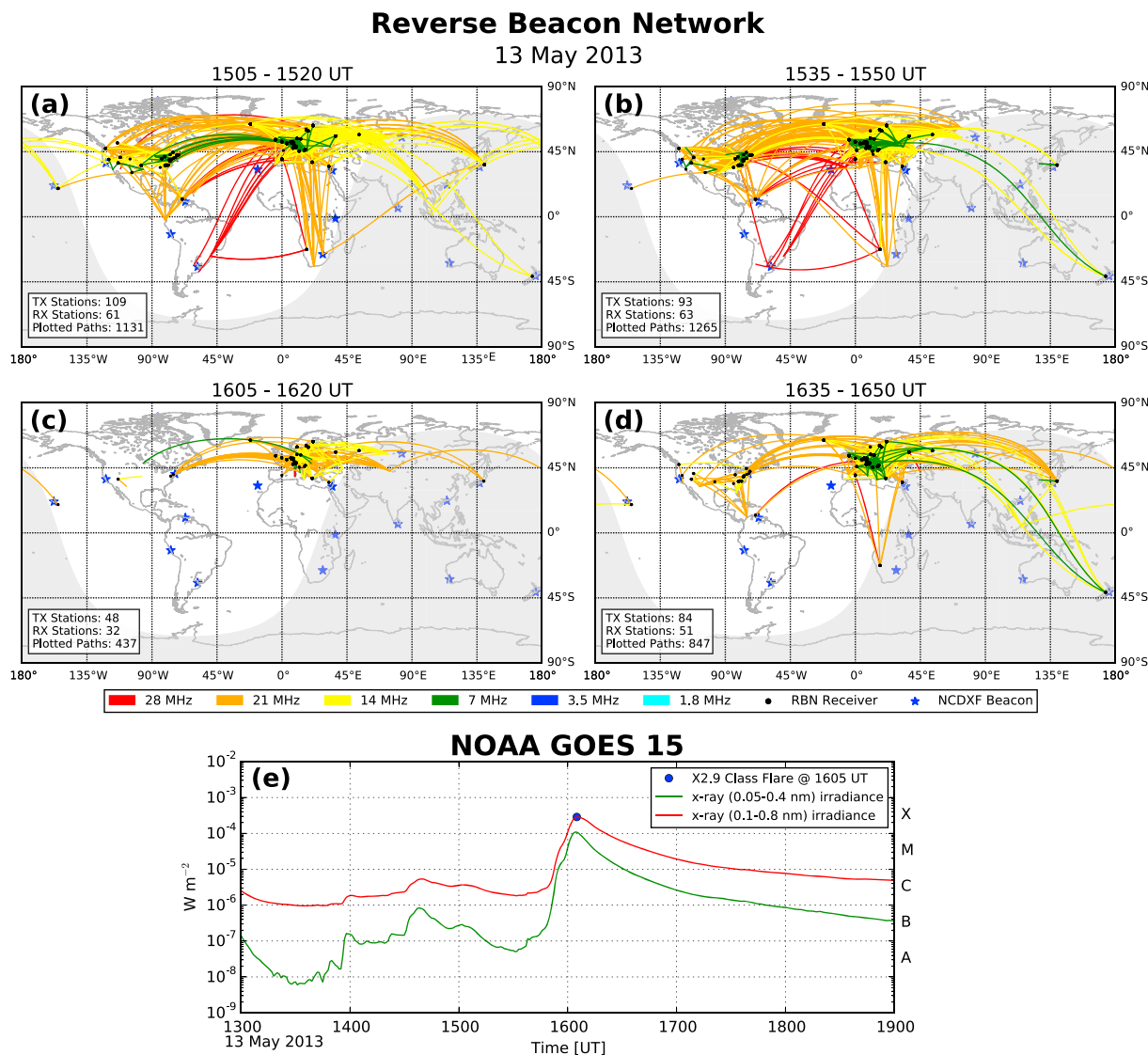


**Figure 3.** (a–d) Reverse Beacon Network (RBN) high-frequency propagation path observations from 13 May 2013 beginning at 1505 UT with 15 min integration periods and a 30 min cadence. Paths are color coded by frequency band. Black dots indicate RBN receiving stations, while blue stars indicate Northern California DX Foundation (NCDXF) beacons. The number of unique transmitting (TX) and receiving (RX) stations within each 15 min period is given in the lower left corner of each map. Shading indicates the solar terminator. (e) GOES 15 X-ray sensor measurements for the 0.05–0.4 nm (green trace) and the 0.1–0.8 nm (red trace) soft X-ray bands for 13 May 2013 1300–1900 UT. A blue dot at 1605 UT on the red trace indicates the peak of an X2.9 class solar flare and corresponds to a dramatic decrease in RBN activity.

beginning at 1505 UT with 15 min integration periods and a 30 min cadence. Observations are color coded by frequency band, with blues and greens indicating lower frequencies (1.8–14 MHz) and yellows and reds indicating higher frequencies (14–28 MHz). Black dots indicate RBN receiving stations, which are only shown if a particular receiving station detects at least one transmitting station during a given integration period. The RBN identifies each station by call sign, which is geolocated via a lookup in the QRZ.com database (<http://www.qrz.com>). RBN observations without valid database locations are omitted from the maps and subsequent analysis. The number of plotted propagation paths, transmitting stations, and receiving stations identified during each integration period is printed in the lower left-hand corner of each map. Shading indicates the location of the solar terminator. The geolocated RBN data presented in Figures 3a–3d are available as Data Set S1 in the supporting information.

Figure 3e shows GOES 15 X-ray sensor [Chamberlin *et al.*, 2009] measurements for the 0.05–0.4 nm (green trace) and the 0.1–0.8 nm (red trace) soft X-ray bands for 13 May 2013 1300–1900 UT. The GOES 15 satellite is

in geostationary orbit at 135°W longitude, and therefore able to observe X-ray flux incident on the daylight region of the RBN maps shown. A blue dot at 1605 UT on the red trace indicates the peak of a sharp increase in X-ray flux indicative of an X2.9 class solar flare. The peak of this flare is observed coincident with the starting time of the Figure 3c RBN map and corresponds to a dramatic decrease in HF propagation conditions observed by the RBN. Figures 3a and 3b show a significant number (over 1100) of HF paths between Europe, North America, South America, and Africa on frequencies from 7 to 28 MHz. Immediately after the peak of the flare, Figure 3c shows less than 35% of the propagation paths of the preceding map. Almost all 7 and 28 MHz activity disappears, along with all links to South America, Africa, and most links between Europe and the United States. Figure 3d, which begins 30 min after the flare peak, starts to show some recovery as a few paths from Europe to the Western United States, South America, and Africa reappear, along with some 7 and 28 MHz activity.

## Discussion

The 13 May 2013 1605 UT solar flare event provides a strong example of the types of monitoring and observations that can be made with the Reverse Beacon Network (RBN). It is also important to discuss factors which may bias the data. One factor possibly apparent from studying the Figure 3 maps is the spatial distribution of transmitters and receivers. Certain geographic regions, such as North America and Europe, tend to have a large number of amateur stations due to both economic and political conditions in those regions. Human behavior also affects the number of signals present at any given time, as transmissions generally require operators to be awake and available during leisure hours. Also, operators will automatically adjust their transmissions to bands which appear to have the best propagation conditions, which can lead to a lack of sampling on frequencies with poor propagation. Amateur networks are also not subject to rigorous station design, which leads to uncertainty of gain, loss, and directivity factors at any given station. Finally, networks which rely on databases for geolocation are subject to incorrect location reporting when amateurs decide to operate from portable stations or fail to update their location when moving.

Although these biases exist, effects of these issues may be mitigated. For instance, the station distribution problem is partially addressed by a large number of radio amateurs who are motivated to operate from remote locations. Both the spatial problem and the human behavior problem are further addressed by the existence of the Northern California DX Foundation (NCDXF) beacon network, a globally distributed set of autonomous Morse code beacons operating on the amateur bands from 14 to 28 MHz [Troster and Fabry, 1997]. These beacons are built to known specifications and transmit on a published schedule from known locations, as indicated by the blue stars in Figures 3a–3d. It is possible to further improve the data through the installation of additional receivers by interested parties such as researchers, as well as improve the capabilities of the skimming software used for automatic observations. Software could be created with capabilities to automatically observe more types of transmissions, including voice communications. With current SDR capabilities, it is also possible to make observations of nonamateur signals via software upgrades to current systems. Good use could then be made of transmitters with known characteristics, such as standards stations and commercial broadcast stations. Finally, careful analysis using all data available, not just that from a single network, will greatly enhance the value of the observations.

## Summary

In this article, we demonstrated the ability of one amateur radio reporting network, the Reverse Beacon Network (RBN), to detect space weather disturbances by examining the impacts on HF propagation of an X2.9 class solar flare detected by the GOES 15 satellite. Prior to the solar flare, the RBN observed strong HF propagation conditions between multiple continents, primarily Europe, North America, and South America. Immediately following the GOES 15 detection of the solar flare, the number of reported global RBN propagation paths dropped to less than 35% that of prior observations. After the flare, the RBN showed the gradual recovery of HF propagation conditions.

Amateur radio reporting networks, such as the RBN, PSKReporter, and WSPRNet are powerful tools for remote sensing the ionosphere. These voluntarily constructed and operated networks provide real-time and archival data that could be used for space weather operations, forecasting, and research. We recognize that the observations made by these networks essentially constitute an untapped “big data” resource in the

fields of space weather and space science, one which merits further exploration. The potential exists for the study of both global and localized effects.

#### Acknowledgments

The RBN data shown in Figure 3 are available as supporting information Data Set S1. The GOES data shown in Figure 3 are provided by the Space Weather Prediction Center, Boulder, Colorado, National Oceanic and Atmospheric Administration (NOAA), U.S. Department of Commerce and are available at <http://satdat.ngdc.noaa.gov>. We acknowledge the use of the free, open source software projects used in this analysis: Ubuntu Linux, python, matplotlib, pandas, NumPy, SciPy, IPython, python-hamtools, and others.

#### References

- Chamberlin, P. C., T. N. Woods, F. G. Eparvier, and A. R. Jones (2009), Next generation X-ray sensor (XRS) for the NOAA GOES-R satellite series, in *Solar Physics and Space Weather Instrumentation III*, edited by S. Fineschi and J. A. Fennelly, vol. 7438, pp. 02-1–02-10, SPIE, San Diego, Calif., doi:10.1117/12.826807.
- Chisham, G., et al. (2007), A decade of the Super Dual Auroral Radar Network (SuperDARN): Scientific achievements, new techniques, and future directions, *Surv. Geophys.*, 28, 33–109, doi:10.1007/s10712-007-9017-8.
- Coster, A., and A. Komjathy (2008), Space weather and the Global Positioning System, *Space Weather*, 6(6), S06D04, doi:10.1029/2008SW000400.
- Eccles, V., H. Vo, J. Thompson, S. Gonzalez, and J. J. Sojka (2011), Database of electron density profiles from Arecibo Radar Observatory for the assessment of ionospheric models, *Space Weather*, 9(1), S01003, doi:10.1029/2010SW000591.
- Hunter, J. D. (2007), Matplotlib: A 2D graphics environment, *Comput. Sci. Eng.*, 9(3), 90–95, doi:10.1109/MCSE.2007.55.
- McKinney, W. (2010), Data structures for statistical computing in python, in *Proceedings of the 9th Python in Science Conference*, edited by S. J. van der Walt and J. Millman, pp. 51–56, SciPy.org, Austin, Tex. [Available at <http://conference.scipy.org/proceedings/scipy2010/mckinney.html>.]
- Millman, K. J., and M. Aivazis (2011), Python for scientists and engineers, *Comput. Sci. Eng.*, 13(2), 9–12, doi:10.1109/MCSE.2011.36.
- Pérez, F., and B. E. Granger (2007), IPython: A system for interactive scientific computing, *Comput. Sci. Eng.*, 9(3), 21–29, doi:10.1109/MCSE.2007.53.
- Reinisch, B. W., X. Huang, I. A. Galkin, V. Paznukhov, and A. Kozlov (2005), Recent advances in real-time analysis of ionograms and ionospheric drift measurements with digisondes, *J. Atmos. Sol. Terr. Phys.*, 67(12), 1054–1062, doi:10.1016/j.jastp.2005.01.009.
- Rideout, W., and A. Coster (2006), *Automated GPS Processing for Global Total Electron Content Data*, 10(3), 219–228, doi:10.1007/s10291-006-0029-5.
- Schunk, R. W., et al. (2014), Ensemble modeling with data assimilation models: A new strategy for space weather specifications, forecasts, and science, *Space Weather*, 12(3), 123–126, doi:10.1002/2014SW001050.
- Taylor, J., and B. Walker (2010), WSPRING around the world, *QST*, 94(11), 30–32.
- Troster, J. G., and R. S. Fabry (1997), The NCDXF/IARU international beacon project, *QST*, 81(9), 47–48.

**Nathaniel A. Frissell**, W2NAF, is a PhD candidate in the Space@Virginia Tech SuperDARN Laboratory in Blacksburg, Virginia.

**Ethan S. Miller**, K8GU, is a member of the professional staff at JHU/APL.

**Stephen Kaeppler**, AD0AE, is a Center for Geospace Postdoctoral Fellow at SRI International in Menlo Park, California.

**Felipe Ceglia**, PY1NB, is a businessman with an interest in information technology and ham radio who lives near Rio de Janeiro, Brazil.

**Dave Pascoe**, KM3T, is an avid ham radio operator and independent computer consultant with a keen interest in radio propagation research.

**Nick Sinanis**, F5VIH/SV3SJ, is an engineer in the Radiocommunication Bureau of the International Telecommunication Union.

**Pete Smith**, N4ZR, is a retired NASA official, long-time amateur radio operator and cofounder of the Reverse Beacon Network.

**Richard Williams**, W3OA, is a retired Air Force Colonel and NASA official who wrote and maintains the software that forwards station received information from CW Skimmer to the Reverse Beacon Network server.

**Alex Shovkopyas**, VE3NEA, is the owner of Afreet Software, Inc.

All authors are amateur radio operators with their amateur radio call sign indicated following their name.